Journal of Applied Polymer Science

Poly(ethylene glycol) crosslinked sulfonated polysulfone composite membranes for forward osmosis

Xiaoli Ding,[1,2] Zhiguang Liu,[3] Mingming Hua,[1,2] Te Kang,[1,2] Xu Li,[1,2] Yuzhong Zhang[1,2]

[1]State Key Laboratory of Separation Membranes and Membrane Processes, Tianjin Polytechnic University, Tianjin 300387, China

[2]Institute of Separation Materials and Process Control, School of Material Science and Engineering, Tianjin Polytechnic University, Tianjin 300387, China

[3]EnerTech Drilling and Production Company, China National Offshore Oil Corporation, Tianjin 300452, China

Correspondence to: X. Ding (E-mail: dingxiaoli@tjpu.edu.cn) and Y. Zhang (E-mail: zhangyz2004cn@163.com)

ABSTRACT: Forward osmosis (FO) membranes were prepared by a coating method with poly(ethylene glycol) crosslinked sulfonated polysulfone (SPSf) as a selective layer. The poly(ether sulfone)/SPSf substrate was prepared by phase inversion. The composite membranes were characterized with respect to membrane chemistry (by attenuated total reflectance/Fourier transform infrared spectroscopy and X-ray photoelectron spectroscopy), hydrophilicity (by static contact angle measurement), and surface morphology (by scanning electron microscopy and atomic force microscopy). The FO performance was also characterized. The effects of the crosslinker concentration on the hydrophilicity and FO performance were investigated. The crosslinked membrane exhibited a high hydrophilicity with a lowest contact angle of 15.5°. Under FO tests, the membranes achieved a higher water flux of 15.2 L m^{-2} h^{-1} when used against deionized water as the feed solution and a 2 mol/L sodium chloride (NaCl) solution as the the draw solution. The membranes achieved a magnesium sulfate rejection of 96% and an NaCl rejection of 55% when used against a 1 g/L inorganic salt solution as the feed solution and a 2 mol/L glucose solution as the draw solution. © 2016 Wiley Periodicals, Inc. J. Appl. Polym. Sci. **2016**, *133*, 43941.

KEYWORDS: coatings; crosslinking; membranes

Received 6 November 2015; accepted 12 May 2016

DOI: 10.1002/app.43941

INTRODUCTION

Water scarcity is a serious worldwide problem, and there is an urgent need for secure and sustainable sources of water. Membrane technologies, such as ultrafiltration, nanofiltration, and reverse osmosis, have been applied to large-scale water and wastewater treatment with the advantage of a low operation cost, small footprint, and so on. In the last decade, forward osmosis (FO) has also developed rapidly for water treatment because of its low energy consumption. One major challenge in the exploration of FO potential as one new water production technology is the inadequacy of commercially available high-performance FO membranes.[1,2] In recent years, a significant portion of research on membrane fabrication has been conducted with the aim of improving the FO process, especially on polyamide (PA) thin-film composite membranes fabricated by interfacial polymerization, because of the high performance of FO membranes. Generally, high-performance FO membranes must have the following characteristics: (1) a thin and highly porous supporting layer for better water transport and low internal concentration polarization, (2) a thin and compact selective layer for high salt rejection and water flux, and (3) reasonably good antifouling properties.[3] Therefore, hydrophilicity is desired in FO membranes, as in other water treatment membranes, to enhance flux and reduce membrane fouling; this also decreases the internal concentration polarization. Hydrophilicity modification of the substrate has mainly been conducted by blending the hydrophilic materials such as sulfonated polymers,[4–9] carboxylated polymers,[10] and nanoparticles,[11–14] with the membrane materials. Some substrate membranes were fabricated by hydrophilic materials, such as cellulose acetate propionate, directly.[15] Research on increasing the hydrophilicity of the selective layer has been relatively less common. Some efforts have been made to coat hydrophilic materials on asymmetric FO membranes.[16,17]

Sulfonated polysulfone (SPSf) is a very popular hydrophilic modifier, and the antifouling activity of SPSf membranes has been reported;[18,19] SPSF has also been used in the substrate of the FO membrane.[4] However, SPSf with high degree of sulfonation (DS) has poor mechanical stability because of high water swelling; this prevents its applications in water and wastewater treatment.[20] The swelling problem of SPSf with a high DS can be overcome by crosslinking, and it has been used to prepare membranes for fuel-cell applications.[21]

In this study, composite membranes were prepared by the coating of poly(ethylene glycol) (PEG)-crosslinked SPSf on laboratory-made poly(ether sulfone) (PES)/SPSf porous substrates. The ether oxygen group improved the hydrophilicity and then the antifouling properties, which have attracted much attention in water treatment membranes.[17,22,23] Castrillón *et al.*[17] fabricated a low-fouling FO membrane by grafting PEG derivatives on PA composite membranes through a dual interfacial reaction. SPSf in the substrate made the substrate more hydrophilic and could crosslink with the crosslinker in the coating solution; this strengthened the conjunction between the supporting substrate and the selective layer. The membranes were investigated by characterization of the structural morphology, hydrophilicity, and FO performance.

EXPERIMENTAL

Materials

PES (Ultrason E3010) was purchased from BASF. SPSf was obtained from Tianjin Normal University (China). Polyvinylpyrrolidone (weight-average molecular weight = 30,000, purity = 99%) was purchased from Shanghai Sunpower New Material Co., Ltd. (China). PEG (weight-average molecular weight = 200, purity = 99%), humic acid (purity = 99%), sodium sulfate (Na_2SO_4; purity = 99%), sodium chloride (NaCl; purity = 99.5%), magnesium sulfate ($MgSO_4$; purity = 98%), and magnesium chloride ($MgCl_2$; purity = 98%) were purchased from Tianjin Guangfu Fine Chemical Research Institute (China). Glucose (Glc; purity = 99%) was purchased from Shanghai Sinopharm Chemical Reagent Co., Ltd. (China). *N,N*-Dimethylacetamide (purity = 99%) was purchased from Tianjin Yingdaxigui Chemical Reagent Plant (China). Isopropyl alcohol (purity = 99.5%) was purchased from Tianjin Fengchuan Chemical Reagent Plant (China). All chemicals were used as received. Deionized (DI) water used in the experiment was self-made in the laboratory.

Fabrication of the Composite Membranes

The PES/SPSf porous membrane used as the substrate was prepared by the Loeb–Sourirajan wet-phase inversion method. The casting solution consisted of 12.6 wt % PES, 8.4 wt % SPSf (DS = 10%), 7 wt % polyvinylpyrrolidone, and 72 wt % *N,N*-dimethylacetamide. The casting solution was cast on a nonwoven fabric that was fixed on a flat glass plate by adhesive tape and was then immersed into DI water to form a porous substrate with a thickness of about 200 μm. The membrane was washed in running water for 48 h to remove the residual solvent. Then, the membrane was dried in air.

The composite membrane was prepared by a coating method. To form the coating solution, SPSf (DS = 50%) with a concentration of 9 wt % was dissolved in a mixture of isopropyl alcohol and DI water to form a homogeneous solution. Then, the crosslinker PEG was added to the stirred solution.

The SPSf concentration in the coating solution (wt $\%_{SPSf}$) was calculated according to the following equation:

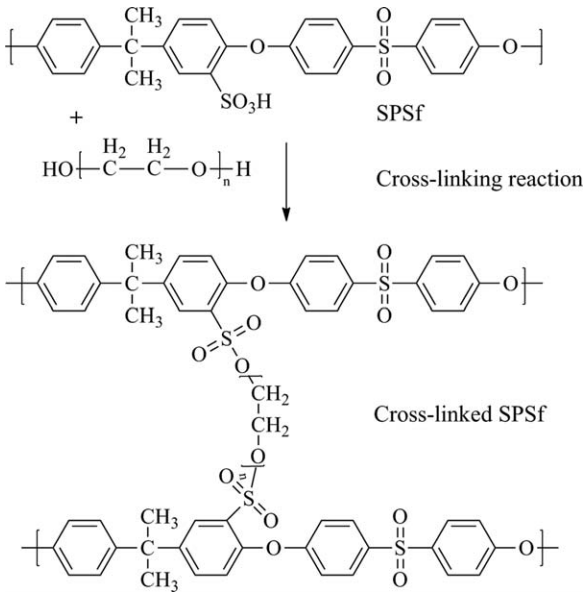

Figure 1. Reaction scheme for SPSf and PEG.

$$\text{wt }\%_{SPSf} = \frac{\text{SPSf weight}}{\text{SPSf weight} + \text{Solvent weight}} \times 100\% \quad (1)$$

The PEG concentration in the coating solution (wt $\%_{PEG}$) was calculated according to the following equation:

$$\text{wt }\%_{PEG} = \frac{\text{PEG weight}}{\text{PEG weight} + \text{SPSf weight} + \text{Solvent weight}} \times 100\% \quad (2)$$

After being degassed, the homogeneous solution containing the SPSf and crosslinker was poured onto the substrate membrane surface, and pressure was applied to the casting ring to create a seal and prevent the solution from leaking around the edge of the casting ring. After 1 min, the coating solution was poured out from the casting ring. After the casting ring was removed, the membrane was suspended perpendicularly in a vacuum oven at 80 °C for 2 h to allow the crosslinking reaction to proceed. The crosslinking reaction between SPSf and PEG is presented in Figure 1.

Characterizations of the Membranes

Attenuated total reflectance/Fourier transform infrared (ATR–FTIR) spectroscopy (Bruker Vector 22, Germany) was used to characterize the chemical structure of the membrane surface. For each measurement, 128 spectra were accumulated from 600 to 4000 cm^{-1} at a resolution of 4 cm^{-1}.

X-ray photoelectron spectroscopy (Thermo Fisher) was used to characterize the surface elemental content of the membrane with a monochromatic AlKα X-ray source (15 kV, 150 W). The surface elemental stoichiometries were determined from the peak area ratios after correction with experimentally determined instrumental sensitivity factors.

The surface hydrophilicity of the membrane was characterized by static contact angle measurement, which was performed by the sessile drop method in a contact angle geniometer (SL200KB, Shanghai Solon, China) with DI water as the probe

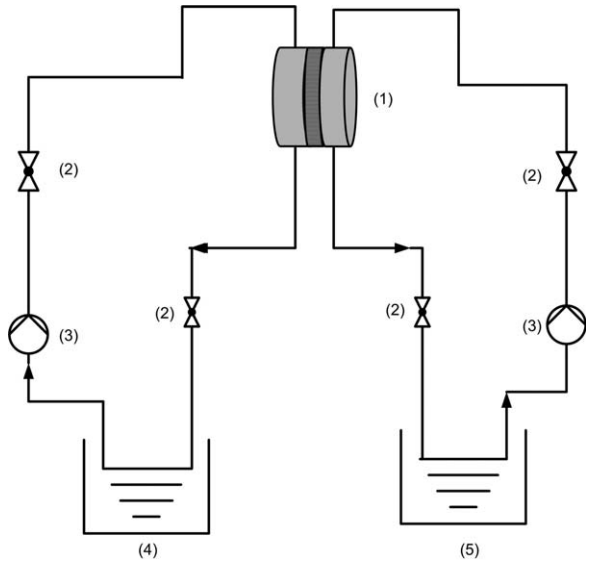

Figure 2. Laboratory-scale FO process: (1) FO flat membrane module, (2) valve, (3) peristaltic pump, (4) draw solution reservoir, and (5) feed solution reservoir.

liquid at room temperature. To minimize the experimental error, the contact angle was randomly measured at more than five different locations for each specimen.

The membrane morphology and topology were examined with field emission scanning electron microscopy (S-4800, Hitachi, Japan) and atomic force microscopy (AFM; 5500AFM/SPM, Agilent). The membrane specimen, which was dried with a freeze dryer (DF-1A-50, Beijing Boyikang, China), was fractured with a sharp razor blade before it was sputtered with gold for the field emission scanning electron microscopy scan. The AFM test was done with tapping mode for a scanned area of 6 × 6 μm^2 at a scanning rate of 1.2 Hz.

FO Performance of the Composite Membranes

The FO performance of the membranes was evaluated by a laboratory-scale filtration unit with a flat membrane area of 20.0×10^{-4} m^2 at room temperature (~25 °C), as shown in Figure 2. All experiments were repeated three times. The flow velocities of the feed and the draw solution during the FO test were kept at 20 L/h for all of the experiments. During the tests, the dilution of the draw solution was ignored because the ratio of the water permeation flux to the volume of the draw solution was less than 1 wt %. The water permeation flux from the feed solution to the draw solution [J_V (L m^{-2} h^{-1})] was calculated from the weight change of the feed water [w (kg)] with a digital mass balance (D10, Shenzhen Xinli Co., China) according to the following equation:

$$J_V = \frac{w/\rho}{At} \tag{3}$$

where ρ is the density of the pure water (kg/L), A is the effective membrane surface area (m^2), and t is the test time (h).

The reverse diffusion of the draw solute (J_{DS}; g m^{-2} h^{-1}) from the draw solution to the feed side was calculated from the concentration increase of the draw solute in the feed solution according to the following equation:

$$J_{DS} = \frac{w_1 c_1 - w_2 c_2}{\rho A t} \tag{4}$$

where w_1 is the weight of the feed water before the test (kg), w_2 is the weight of the feed water after the test (kg), c_1 is the concentration of the draw solute in the feed water before the test (g/L), and c_2 is the concentration of the draw solute in the feed water after the test (g/L). The salt concentration was determined from the conductivity measurement by electrical conductivity (DDS-11A, Shanghai Hongyi Instrument Co., Ltd., China). The Glc concentration was determined by the measurement of the absorbance at 630 nm with an ultraviolet–visible spectrophotometer (UV-2450, Shimadzu Co., Japan) after *ortho*-toluidine complexation.

The rejection ratio (R) was calculated with the following equation:

$$R(\%) = \left(1 - \frac{c_{DS}}{c_f}\right) \times 100\% \tag{5}$$

where c_{DS} and c_f are the concentrations of the reject in the draw solution side and the feed side after the test, respectively.

RESULTS AND DISCUSSION

Characterization of the Membranes

The chemical structure of the crosslinked skin of the composite membrane was confirmed by ATR–FTIR spectroscopy, as shown in Figure 3. The characteristic peaks corresponding to —SO_3H group were observed at 1027 and 1197 cm^{-1} in SPSf[24,25]; these were absent in the crosslinked SPSf skin. Crosslinking was also confirmed by the presence of the characteristic peak from 3000 to 2800 cm^{-1}, which represented the various C—H stretching frequencies for methyl and methylene groups present in PEG.[9]

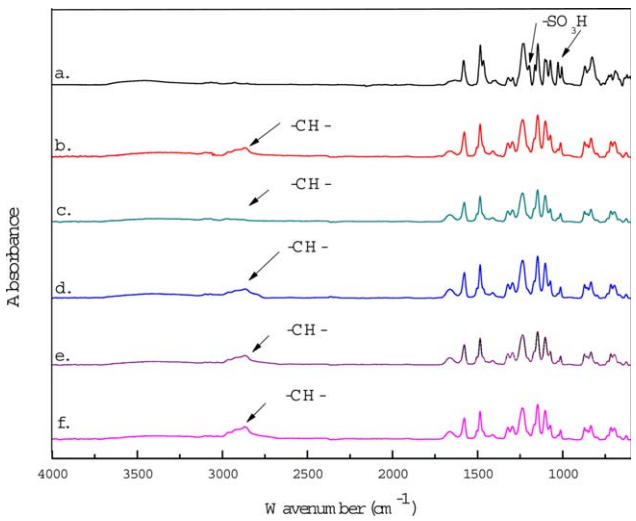

Figure 3. ATR–FTIR spectra for the uncrosslinked and crosslinked skins of the composite membranes: (a) SPSf, (b) 1 wt % crosslinker concentration, (c) 3 wt % crosslinker concentration, (d) 5 wt % crosslinker concentration, (e) 7 wt % crosslinker concentration, and (f) 9 wt % crosslinker concentration. [Color figure can be viewed in the online issue, which is available at www.interscience.wiley.com.]

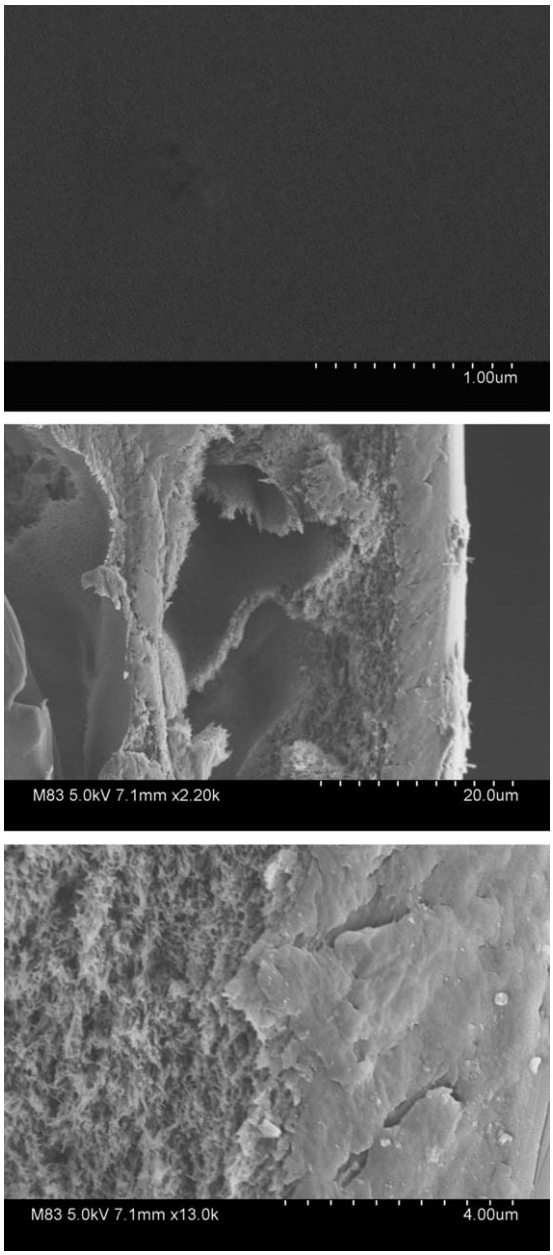

Figure 4. Scanning electron microscopy images of the surface and cross-sectional morphology.

There was no significant morphological variation between the crosslinked membranes in the scanning electron microscopy images. The typical morphology of the composite membrane is depicted in Figure 4. The composite membrane consisted of a dense symmetric skin (ca. 7 μm in thickness for the specimen) and an asymmetric supporting layer. The coating layer was homogeneously coated on the supporting membrane without the characteristics of asymmetric membranes but with a uniform structure; this is the natural structure formed by the solvent evaporation method. The surface morphology of the membrane was smooth and flat; no cracks or big holes were observed on the membrane surface. The cross-sectional images exhibited the typical asymmetric structure. The supporting layer had a small portion of spongelike structure (ca. 5 μm in thickness) beneath the top surface layer and a macrovoid structure with good interconnection near the nonwoven fabric layer. The big pores observed on the bottom surface mitigated the internal concentration polarization effect within the porous substrate. The distinguishable boundary between the coating layer and the substrate is illustrated in Figure 4, and the adhesion of the coating layer to the substrate was excellent; no obvious delamination existed.

The AFM images (Figure 5) clearly compared the top surfaces of the membranes. The surface roughness, which was expressed in terms of the mean roughness (R_a), showed a sharp decrease after the PES/SPSf substrate was coated. The substrate membrane exhibited the highest roughness. The coating created a smoother membrane surface on the substrate. With increasing crosslinker content, R_a decreased and then increased. The membrane crosslinked with 5 wt % PEG exhibited the lowest roughness; this indicated that the membrane had the smoothest surface, and this was due to the sufficient coverage on the membrane surface. When the crosslinker increased to 7 or 9 wt %, the fluidity and extensibility of the coating solution weakened, and this increased the roughness.

The contact angle values are presented in Figure 6. The results show that the crosslinking of SPSf with PEG enhanced the hydrophilicity by lowering the contact angle from 64.3 to 15.5°. The initial contact angle had a higher value than that after 30 s. The most probable reason for the contact angle decrease was the increase in the hydrophilicity. The change in the contact angle was effected by many factors, including swelling and dissolution. In this study, the membrane skin was compact, and the porosity–permeability effect was negligible. The membrane without crosslinking suffered the most serious swelling, but the decrease in the contact angle with time was negligible. This indicated that the decrease in the contact angle for the crosslinking membrane was not induced by swelling because the swelling was suppressed by crosslinking. The changes in the water drop volumes at 30 s are presented in Figure 7. The water droplet volumes on the uncrosslinked membrane were found to change insignificantly, as shown in Figure 7(A); this also indicated that the effect of evaporation on the droplet volume could be neglected. The water droplet volumes on the PEG-crosslinked membranes were found to decrease, as shown in Figure 7(B–F). The most probable reason for the decrease in the water droplet volume could have been the adsorption of the water by the hydrophilic skin because the evaporation, swelling, and porosity–permeability effect could be neglected. We presumed that in the membrane skin fabricated by the solvent evaporation method, the PEO segment was embedded in the membrane; after the membrane came into contact with the water, the PEO segment chain migrated to the membrane surface by surface segregation to minimize the interfacial free energy. The surface elemental compositions from the X-ray photoelectron spectroscopy survey scan of the membranes at the initial time and after wetting are presented in Table I. It was clear that there was an obviously higher value of O atomic concentration in the wetted crosslinked membrane; this indicated that the PEO segments were extended to the membrane surface.

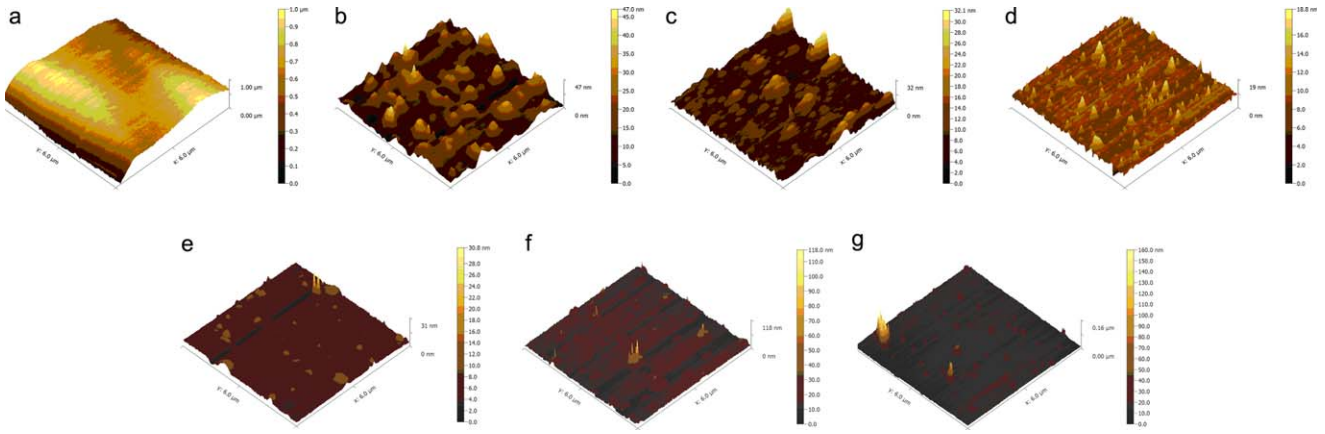

Figure 5. Three-dimensional AFM images of (A) the substrate membrane, (B) the membrane without crosslinking, (C) the membrane crosslinked with 1 wt % PEG, (D) the membrane crosslinked with 3 wt % PEG, (E) the membrane crosslinked with 5 wt % PEG, (F) the membrane crosslinked with 7 wt % PEG, and (G) the membrane crosslinked with 9 wt % PEG. [Color figure can be viewed in the online issue, which is available at wileyonlinelibrary.com.]

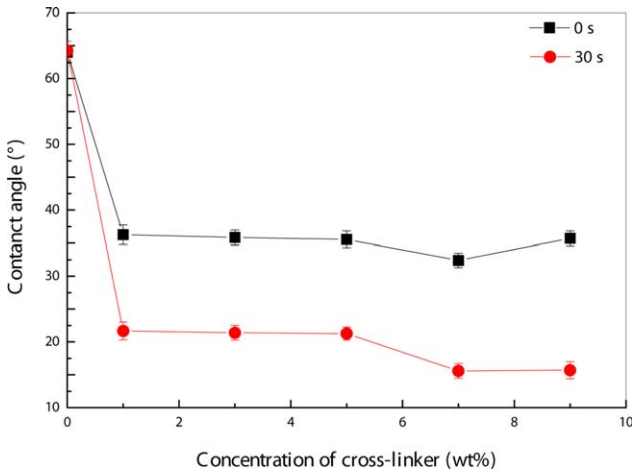

Figure 6. Contact angle values of the composite membrane skins. [Color figure can be viewed in the online issue, which is available at wileyonlinelibrary.com.]

The concentration of the hydrophilic functional groups at the reconstructed surface enhanced the hydrophilicity; then, the contact angle decreased as the time increased.[26,27]

FO Performance of the Composite Membranes

The FO water permeation flux and J_{DS} for the membranes with DI water as the feed solution are shown in Figures 8 and 9. The water permeation flux and J_{DS} decreased with increasing crosslinker concentration because of the higher crosslinking density and more compact skin (Figure 8). Although the membrane without crosslinking had a lower J_{DS} for inorganic salt than the crosslinked membrane with 1 wt % PEG in crosslinking solution, the membrane without crosslinking was electronegative because of the $-SO_3^-$ group, and the electrostatic effect decreased J_{DS}. When different draw solutes were used, the water permeation fluxes decreased in the following order: $MgCl_2 > Na_2SO_4 > NaCl > MgSO_4 > Glc$ [Figure 8(A)]; this was because, at the same molecular concentration, the osmotic pressures of several solutions decreased in the following order:

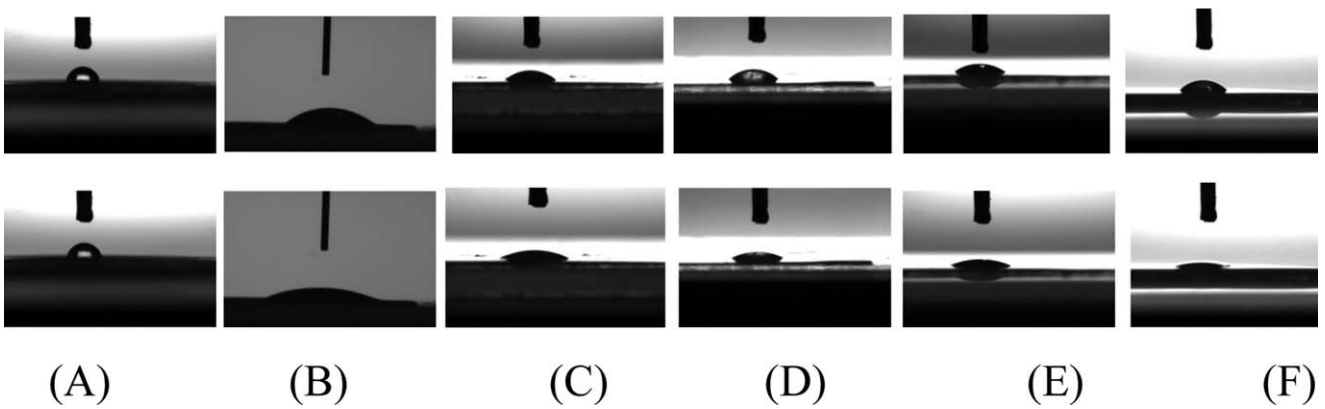

Figure 7. Images of droplets corrected at the initial time and after 30 s: (A) on the membrane without crosslinking, (B) on the membrane crosslinked with 1 wt % PEG, (C) on the membrane crosslinked with 3 wt % PEG, (D) on the membrane crosslinked with 5 wt % PEG, (E) on the membrane crosslinked with 7 wt % PEG, and (F) on the membrane crosslinked with 9 wt % PEG.

Table I. Surface Elemental Compositions of the Membranes

Membrane	Surface elemental composition (mol %)	
	O	C
Dry membrane crosslinked with 1 wt % PEG	20.33	63.37
Wetted membrane crosslinked with 1 wt % PEG	21.36	62.99
Dry membrane crosslinked with 3 wt % PEG	22.93	58.01
Wetted membrane crosslinked with 3 wt % PEG	24.03	57.87

$MgCl_2 > Na_2SO_4 > NaCl > MgSO_4 > Glc$.[2,28] The water permeation flux increased with increasing draw solute concentration because a larger effective osmotic pressure provided a greater driving force [Figure 9(A)]. J_{DS} decreased as follows: $NaCl > MgCl_2 > Na_2SO_4 > MgSO_4 > Glc$ [Figure 8(B)]. The reverse diffusion of Glc had the lowest value because of the largest molecular size. For the inorganic ions, the hydrated radius decreased as follows: $Mg^{2+} > SO_4^{2-} > Na^+ > Cl^-$,[29] the reverse diffusion of $MgSO_4$ had the lowest value among the four inorganic salts, and that of NaCl had the highest value. Because Cl^- had the smallest hydrated radius, the reverse diffusion of $MgCl_2$ had a higher value than that of Na_2SO_4 as a result of the Donnan equilibrium. The experiment results showed that small molecular organic compounds, such as Glc, were more suitable as draw solutes in this process. The inorganic salt had a high reverse diffusion because of its small hydrated radius and the loss of the charge induced by the crosslinking reaction between —SO_3H and —OH. The reverse diffusion also decreased with decreasing concentration of the draw solute [Figure 9(B)] because of the lower driving force produced by the concentration difference.

Table II presents the desalination performance of the membrane with 5 wt % PEG-crosslinked SPSf in the coating solution with the 2 mol/L Glc solution as the draw solution and the 1 g/L NaCl solution and 1 g/L $MgSO_4$ solution as the feed solution. The water permeation flux decreased compared to that when DI water was used as the feed solution. This was due to the reduction in the effective driving force that was due to NaCl and $MgSO_4$ in the feed solution. The membrane had a higher $MgSO_4$ rejection (96%) than NaCl rejection (55%).

Humic acid was used as a model foulant for the fouling test. The membrane without crosslinking and the membranes crosslinked with 1 and 9 wt % PEG were evaluated under the

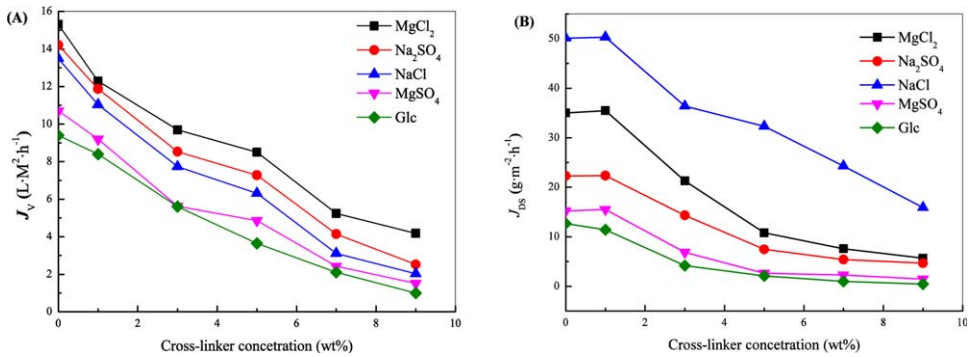

Figure 8. FO water permeation flux and J_{DS} for membranes with different crosslinker concentrations for different draw solutes. The testing conditions were DI water as the feed solution and $MgCl_2$, Na_2SO_4, NaCl, $MgSO_4$, and Glc as the draw solutes at a concentration of 1 mol/L. The flow velocities of the feed and the draw solution during the FO test were kept at 20 L/h. [Color figure can be viewed in the online issue, which is available at wileyonlinelibrary.com.]

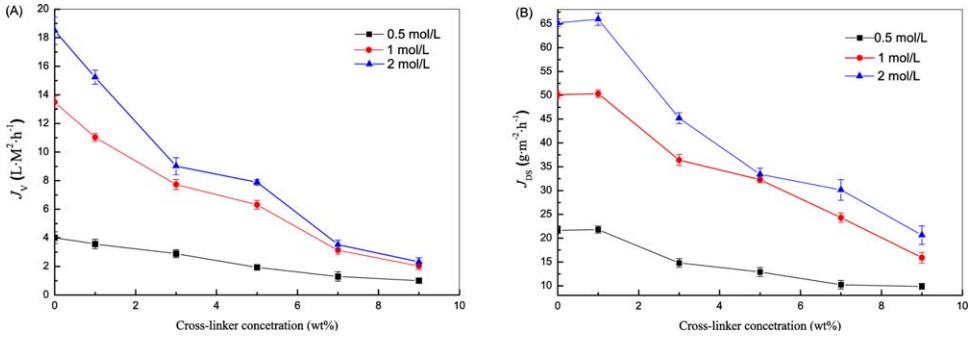

Figure 9. FO water permeation flux and J_{DS} for membranes with different crosslinker concentrations for different draw solution concentrations. The testing conditions were DI water as the feed solution and NaCl as the draw solute. The flow velocities of the feed and the draw solution during the FO test were kept at 20 L/h. [Color figure can be viewed in the online issue, which is available at wileyonlinelibrary.com.]

Table II. Desalination Performance of the Composite Membranes

Feed solute	Water permeation flux (L m^{-2} h^{-1})	Reverse diffusion (g m^{-2} h^{-1})	Salt rejection (%)
$MgSO_4$	5.0	1.2	96
NaCl	6.5	1.5	55

The membrane surface was crosslinked with 5 wt % PEG. The testing conditions were NaCl and $MgSO^4$ solutions as the feed solutions at a concentration of 1 g/L and Glc as the draw solute at a concentration of 2 mol/L. The flow velocities of the feed and the draw solutions during the FO test were kept at 20 L/h.

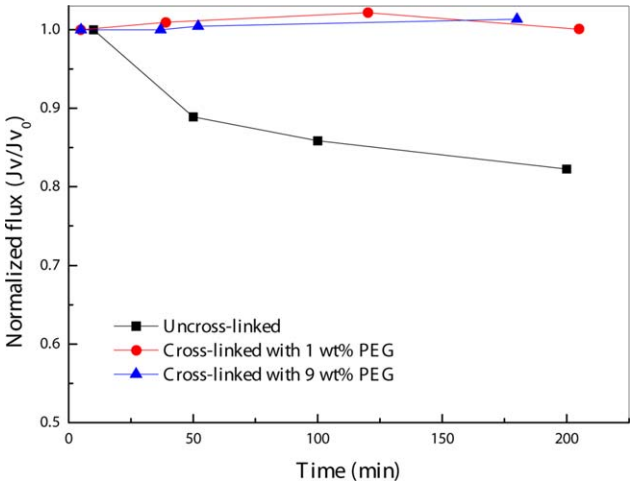

Figure 10. FO normalized water permeation flux for 3.5 h of filtration of a 100 ppm humic acid solution. JV_0:JV in initial. [Color figure can be viewed in the online issue, which is available at wileyonlinelibrary.com.]

following conditions: a 100-ppm humic acid solution was used as the feed and 1 mol/L $MgSO_4$ was used as the draw solution. As shown in Figure 10, there was a flux decline for the uncrosslinked membrane during the FO test, whereas the flux of the crosslinked membranes remained the same as the water permeation flux for the first 3.5 h of the FO filtration. The results demonstrate that an improvement in the antifouling properties compared to those of the uncrosslinked membrane was observed.

The performance of some of the reported FO membranes are listed in Table III. The membranes prepared by the coating method in this study exhibited a higher reverse diffusion of NaCl than others and a little higher water permeation flux than commercial HTI flat sheet membranes, whereas they exhibited lower values than PA-based composite membranes in other literature. The high reverse diffusion of NaCl was the result of the absence of the surface charge due to crosslinking. The difference in the water permeation fluxes between the coated membranes and the PA-based composite membranes was mainly due to the difference in the membrane thickness of the dense layer. The dense layer of the membrane in this study had a thickness of about 7 μm (Figure 4); this resulted in a high mass-transfer resistance. Although the PA-based composite membrane prepared by interfacial polymerization was thinner, with a thickness of even less than 0.1 μm, the major challenge for coated membranes in the future is to reduce the thickness of the dense layer.

CONCLUSIONS

Composite membranes prepared by the coating of a PEG-crosslinked SPSf solution on a PES/SPSf substrate were used as FO membranes. The membranes had a typical asymmetric structure with a dense selective layer on a porous substrate. The

Table III. Comparison of the FO Membrane Performances

Membrane	Material for selective layer	Membrane thickness	J_W (L m^{-2} h^{-1})	J_{DS} (g m^{-2} h^{-1})	Reference
Commercial HTI membrane (flat sheet)	Cellulose triacetate	50 μm[a]	13.0	10.5	30
PA-based composite membrane (flat sheet)	PA polymerized by *p*-phenylenediamine and 1,3,5-trimesoylchloride	150 nm[b]	26.0	8.3	4
PA-based composite membrane (flat sheet)	PA polymerized by *m*-phenylenediamine and glycerol	1 μm[b]	76.3	11.8	3
PA-based composite membrane (hollow fiber)	PA polymerized by *m*-phenylenediamine and trimesoylchloride	300 nm[b]	22.5	2.5	31
Double dense-layer membrane (flat sheet)	Cellulose acetate	1.02 ± 0.08 μm/95 ± 7 nm[b]	10.3	0.8	32
Coated composite membrane (flat sheet)	PEG-crosslinked SPSf	7 μm[b]	15.2	65.9	This work

The feed solution was DI water, and the draw solution was a 2 mol/L NaCl solution.
[a] For the total membrane.
[b] For the selective layer.

membranes had a hydrophilic skin with a lowest water contact angle of 15.5°, and the substrate also was made hydrophilic by the blending of SPSf. Crosslinking with PEG decreased the water contact angle and the fouling trend. The water permeation flux and J_{DS} decreased with increasing crosslinking density. Compared with FO membranes prepared by interfacial polymerization, the coated membranes had a lower water permeation flux because of the thicker dense layer and a higher J_{DS}. The coated membrane was more suitable for use in removal wastewater treatments, such as dye removal in wastewater treatment, than desalination because of the higher reverse diffusion of univalent ions. In the initial stage, the coated membrane could not compete with the membranes prepared by interfacial polymerization in the FO performance. However, this study provided a new way to fabricate hydrophilic FO membranes with a stable mechanical strength and improved antifouling properties. Further research should be conducted to densify and thin the membrane skin.

ACKNOWLEDGMENTS

The authors sincerely thank the National Natural Science Foundation of China (grants 21206121, 51373120, 51173132, and 21274108), the Tianjin City High School Science and Technology Fund Planning Project (grant 20090514), the Tianjin Training Program of Innovation and Entrepreneurship for Undergraduates (grant 201510058067), and the Science and Technology Plans of Tianjin (grant 15PTSYJC00230) for financially supporting this study.

REFERENCES

1. Zhao, S.; Zou, L.; Tang, C. Y.; Mulcahy, D. *J. Membr. Sci.* **2012**, *396*, 1.
2. Cath, T. Y.; Childress, A. E.; Elimelech, M. *J. Membr. Sci.* **2006**, *281*, 70.
3. Ong, R. C.; Chung, T. S.; De Wit, J. S.; Helmer, B. J. *J. Membr. Sci.* **2015**, *473*, 63.
4. Wang, K. Y.; Chung, T. S.; Amy, G. *AIChE J.* **2012**, *58*, 770.
5. Zhong, P.; Fu, X.; Chung, T. S.; Weber, M.; Maletzko, C. *Environ. Sci. Technol.* **2013**, *47*, 7430.
6. Han, G.; Chung, T. S.; Toriida, M.; Tamai, S. *J. Membr. Sci.* **2012**, *423*, 543.
7. Peyravi, M.; Rahimpour, A.; Jahanshahi, M.; Javadi, A.; Shockravi, A. *Micropor. Mesopor. Mater.* **2012**, *160*, 114.
8. Sundell, B. J.; Jang, E.; Freeman, B. D.; Cook, J.; Riffle, J. S.; Mcgrath, J. E. *Ind. Eng. Chem. Res.* **2016**, *55*, 1419.
9. Tripathi, B. P.; Dubey, N. C.; Stamm, M. *J. Membr. Sci.* **2014**, *453*, 263.
10. Cho, Y. H.; Han, J.; Han, S.; Guiver, M. D.; Park, H. B. *J. Membr. Sci.* **2013**, *445*, 220.
11. Emadzadeh, D.; Lau, W. J.; Matsuura, T.; Hilal, N.; Ismail, A. F. *Desalination* **2014**, *348*, 82.
12. Niksefat, N.; Jahanshahi, M.; Rahimpour, A. *Desalination* **2014**, *343*, 140.
13. Yin, J.; Deng, B. *J. Membr. Sci.* **2015**, *479*, 256.
14. Vatanpour, V.; Shockravi, A.; Zarrabi, H.; Nikjavan, Z.; Javadi, A. *J. Ind. Eng. Chem.* **2015**, *30*, 342.
15. Li, X.; Wang, K. Y.; Helmer, B.; Chung, T. S. *Ind. Eng. Chem. Res.* **2012**, *51*, 10039.
16. Ahn, H. R.; Tak, T. M.; Kwon, Y. N. *Desalination Water Treat.* **2015**, *53*, 1.
17. Romero-Vargas Castrillón, S.; Lu, X.; Shaffer, D. L.; Elimelech, M. *J. Membr. Sci.* **2014**, *450*, 331.
18. Chen, M. H.; Chiao, T. C.; Tseng, T. W. *J. Appl. Polym. Sci.* **1996**, *61*, 1205.
19. Malaisamy, R.; Mahendran, R.; Mohan, D.; Rajendran, M.; Mohan, V. *J. Appl. Polym. Sci.* **2002**, *86*, 1749.
20. Noshay, A.; Robeson, L. M. *J. Appl. Polym. Sci.* **1976**, *20*, 1885.
21. Yuan, S.; Yan, G. W.; Xia, Z. J.; Guo, X. X.; Fang, J. H.; Yang, X. H. *High Perform. Polym.* **2014**, *26*, 212.
22. Yu, H. J.; Cao, Y. M.; Kang, G. D.; Liu, Z. N.; Kuang, W.; Liu, J. H.; Zhou, M. Q. *J. Appl. Polym. Sci.* **2015**, *132*, DOI: 10.1002/app.41870.
23. Kim, H. W.; Lee, H. D.; Jang, S. J.; Park, H. B. *J. Appl. Polym. Sci.* **2015**, *132*, DOI: 10.1002/app.41661.
24. Yu, J. J. M. S. Thesis, Hubei University, **2009**.
25. Hu, J. H.; Zhen, X. F. Practical Infrared Spectroscopy; Science: Beijing, **2011**; p 363.
26. Carey, D. H.; Grunzinger, S. J.; Ferguson, G. S. *Macromolecules* **2000**, *33*, 8802.
27. Zhang, Y.; Su, Y. L.; Chen, W. J.; Peng, J. M.; Dong, Y. N.; Jiang, Z. Y.; Liu, H. Z. *J. Membr. Sci.* **2011**, *382*, 300.
28. Shi, Q. M.S. Thesis, Qingdao University of Science and Technology, **2012**.
29. Volkov, A. G.; Paula, S.; Deamer, D. W. *Bioelectrochem. Bioenerg.* **1997**, *42*, 153.
30. Phillip, W. A.; Yong, J. S.; Elimelech, M. *Environ. Sci. Technol.* **2010**, *44*, 5170.
31. Wang, R.; Shi, L.; Tang, C. Y.; Chou, S.; Qiu, C.; Fane, A. G. *J. Membr. Sci.* **2010**, *355*, 158.
32. Zhang, S.; Wang, K. Y.; Chung, T. S.; Chen, H.; Jean, Y. C.; Amy, G. *J. Membr. Sci.* **2010**, *360*, 522.